AUT Journal of Mechanical Engineering

AUT J. Mech. Eng., 1(2) (2017) 243-246
DOI: 10.22060/mej.2017.11892.5209

Phase Field Method to the Interaction of Phase Transformations and Dislocations at Nanoscale

M. Javanbakht[1*], V. I. Levitas[2]

[1] Department of Mechanical Engineering, Isfahan University of Technology, Isfahan 84156-83111, Iran
[2] Iowa State University, Departments of Mechanical and Aerospace Engineering, Ames, IA, USA

ABSTRACT: In this paper, a new phase field method for the interaction between martensitic phase transformations and dislocations is presented which is a nontrivial combination of the most advanced phase field methods to phase transformations and dislocation evolution. Some of the important points in the model are the multiplicative decomposition of deformation gradient into elastic, transformational and plastic parts, defining a proper energy to satisfy thermodynamic equilibrium and instability conditions, including phase-dependent properties of dislocations. The system of equations consists of coupled elasticity and phase field equations of phase transformations and dislocations. Finite element method is used to solve the system of equations and applied to study the growth and arrest of martensitic plate and the evolution of dislocations and phase in a nanograined material. It is found that dislocations play a key role in eliminating the driving force of the plate growth and their arrest which creates athermal friction. Also, the dual effect of plasticity on phase transformations is revealed; due to dislocations pile-up and its stress concentration, the phase transformation driving force increases and consequently, martensitic nucleation occurs. On the other hand, the dislocation nucleation results in decreasing the phase transformation driving force and consequently, the phase transformation is suppressed.

Review History:

Received: 17 August 2017
Revised: 8 March 2017
Accepted: 16 July 2017
Available Online: 21 October 2017

Keywords:

Phase field
Interaction
Phase transformations
Dislocations
Nanoscale

1- Introduction

The interaction between martensitic Phase Transformations (PTs) and dislocations is of great importance for various applications such as transformation-induced plasticity [1], plastic shear-induced PTs under high pressure [2,3], martensite nucleation and growth [4,5,6], and heat and thermomechanical treatments of steels. The main focus of the current paper is on PFA to the interaction between evolving martensitic PTs and discrete dislocations at the nanoscale. Martensitic nucleation in the presence of stationary dislocations was studied by Wand and Khachaturyan [7]. The evolution of martensite (M) with dislocations located at the moving phase interface was treated in Kundin et al. study [8]. A simplified version of a PFA for discrete dislocation theory with martensitic PTs is presented by Levitas and Javanbakht [9]. Here, we combine the most advanced and the only available large-strain PFA with multivariant martensitic PTs [10] and dislocation evolutions [9] and include their nontrivial interactions. For compactness, the single martensitic variant is treated. The FEM simulations are applied to study the growth and arrest of the martensitic plate for temperature-induced PTs, the evolution of dislocations and high-pressure phase in a nanograined material under pressure and shear, and inheritance of dislocations of martensite in austenite for stress-induced PT. Some preliminary results are presented in [11, 12].

2- Complete System of Equations

The following multiplicative decomposition of the deformation gradient F into elastic F_e, transformational U_t, and plastic F_p contributions is justified: $F=F_e \cdot U_t \cdot F_p$. In order to satisfy thermodynamic equilibrium and instability conditions, U_t vs. the order parameter η for a single martensitic variant is accepted as in [10]:

$$\boldsymbol{U}_t = \boldsymbol{I} + \left[a\eta^2(1-\eta)^2 + \left(4\eta^3 - 3\eta^4\right)\right]\varepsilon_t; \quad 0 < a < 6, \tag{1}$$

where ε_t is the transformation strain tensor and I is the unit tensor. For multiple slip systems, an additivity of the plastic velocity gradients for different slip systems is accepted, like in crystal plasticity:

$$l_p := \dot{F}_p . F_p^{-1} := \sum_{\alpha=1}^{p} \frac{1}{H^\alpha} b^\alpha \otimes n^\alpha \dot{\mathrm{Y}}(\xi_\alpha) = \sum_{\alpha=1}^{p} \gamma_\alpha m^\alpha \otimes n^\alpha \dot{\mathrm{Y}}(\xi_\alpha); \quad \mathrm{Y} = (\bar{\xi}_\alpha)^2\left(3 - 2\bar{\xi}_\alpha\right) + Int(\xi_\alpha). \tag{2}$$

Here ξ_α is the order parameter for a dislocation in a slip system α, which varies between n-1 and n when n-1 complete dislocations exist and the n_{th} dislocation appears; $Int(\xi_\alpha)$ and $\bar{\xi}_\alpha$ are the integer and the fractional parts of ξ_α, respectively; b^α is the Burgers vector of the slip system α, H^α is the height of dislocation, n^α is the unit vector normal to the slip system, m^α is the unit vector in the direction of b^α, and $\gamma_\alpha = b^\alpha / H^\alpha$ is the plastic shear strain. The Helmholtz free energy per unit mass can be expressed as the sum of elastic energy ψ^e, thermal energy for PT ψ_η^θ, crystalline energy for dislocations ψ_ξ^c, the energy of interaction of dislocation cores belonging to different slip systems ψ_ξ^{int}, and gradient energies related to martensitic PT ψ_η^∇ and dislocations ψ_η^∇ as follows

Corresponding author, E–mail: javanbakht@cc.iut.ac.ir

$$\psi = J_t \psi^e + \psi_\eta^\theta + \psi_\xi^c + \psi_\xi^{int} + \psi_\eta^\nabla + \psi_\xi^\nabla \tag{3}$$

The elastic energy is

$$\rho_0 \psi^e = \frac{1}{2} \boldsymbol{E}_e : \boldsymbol{C} : \boldsymbol{E}_e \tag{4}$$

where C is the fourth-rank elastic moduli tensor and E_e=1/2(F_e^T. F_e-I) is the Lagrangian elastic strain tensor. Also, J_t=detU_t is the determinant of U_t. The thermal energy is derived as

$$\rho_0 \psi_\eta^\theta = A_0 (\theta - \theta_c) \eta^2 (1-\eta)^2 - \Delta s (\theta - \theta_e)(4\eta^3 - 3\eta^4) \tag{5}$$

where θ_c is critical temperature at which stress-free A loses its stability, θ_e is equilibrium temperature, Δs is the jump in entropy, and A_0 is a parameter. The crystalline energy for dislocations is accepted as follows

$$\begin{aligned}
&\rho_0 \psi_\xi^c = \sum_{\alpha=1}^{p} A_\alpha (\eta, \bar{y}^\alpha)(\bar{\xi}_\alpha)^2 (1-\bar{\xi}_\alpha)^2; \\
&A_\alpha(\eta) = A_\alpha + (A_\alpha^M - A_\alpha^A)\eta^2(3-2\eta); \\
&A_\alpha(\bar{y}^\alpha) = \begin{cases} \bar{A}_\alpha & \bar{y}^\alpha \le H^\alpha; \\ k\bar{A}_\alpha & \bar{y}^\alpha > H^\alpha; \end{cases} \\
&\bar{y}^\alpha = y^\alpha - Int\left(\frac{y^\alpha}{H^\alpha + d^\alpha}\right)(H^\alpha + d^\alpha),
\end{aligned} \tag{6}$$

in which PTs and the inheritance of slip systems during PTs are taken into account. The coefficient $A_\alpha(\eta,\bar{y}^\alpha)$ characterizes the phase dependent theoretical yield strength. It is a periodic step-wise fucntion of the coordinate y^α along the normal to the corresponding slip plane α. The parameter A_α is equal to its normal value $\bar{A}_\alpha$ within each dislocation band of the height H^α and $k\bar{A}_\alpha$ (k >>1) in a thin boundary layer between dislocations of the width d^α. Thus, it excludes the spreading of the dislocation outside the desired dislocation band. The energy of interaction of dislocation cores belonging to different slip systems is expressed in the following form:

$$\begin{aligned}
&\rho_0 \psi_\xi^{\text{int}} = \sum_{\alpha=1}^{p} A_{\alpha k}(\eta)(\bar{\xi}_\alpha)^2 (1-\bar{\xi}_\alpha)^2 (\bar{\xi}_k)^2 (1-\bar{\xi}_k)^2; \\
&A_{\alpha k}(\eta) = A_{\alpha k}^A + (A_{\alpha k}^M - A_{\alpha k}^A)\eta^2(3-2\eta), \\
&A_{\alpha\alpha} = 0.
\end{aligned} \tag{7}$$

where $A_{\alpha k}{}^A$ and $A_{\alpha k}{}^M$ are the coefficients of the energy of interaction of dislocation cores in the austenite (A) and M, respectively. This interaction energy term ensures that dislocations do not simultaneously pass through the same material point. For PTs with only one martensitic variant, the gradient energy can be written as follows:

$$\rho_0 \psi_\eta^\nabla = \frac{\beta_\eta}{2} |\nabla \eta|^2, \tag{8}$$

where β_η is the coefficient of the gradient energy for PT. For dislocations, the gradient energy can be written based on the form in [9] but by considering different coefficients for different phases

$$\begin{aligned}
&\rho_0 \psi_\xi^\nabla = \frac{\beta_\xi(\eta)}{2} \sum_{\alpha=1}^{p} ((\nabla^m \xi_\alpha)^2 + M(1-\bar{\xi}_\alpha)^2 (\nabla^n \xi_\alpha)^2); \\
&\beta_\eta(\eta) = \beta_\xi^A + (\beta_\xi^M - \beta_\xi^A)\eta^2(3-2\eta),
\end{aligned} \tag{9}$$

where $\beta_\xi{}^A$ and $\beta_\xi{}^M$ are the coefficients of the gradient energy for dislocations in A and M, respectively; M is the ratio of the coefficients for the gradient energy normal to and along the slip plane; ∇^m and ∇^n are the gradient operators along and normal to the slip system α, respectively.

The Ginzburg-Landau equations for PTs and dislocations at large strains are expressed as

$$\begin{aligned}
&\dot{\eta} = L^\eta \left(\frac{1}{\rho_0} \boldsymbol{P}^T \cdot \boldsymbol{F}_e : \frac{\partial \boldsymbol{U}_t}{\partial \eta} \cdot \boldsymbol{F}_p + \nabla \cdot \left(\frac{\partial \psi}{\partial \nabla \eta} \right) - \frac{\partial \psi}{\partial \eta} \right); \\
&\dot{\xi}_\alpha = L_\alpha^\xi(\eta) \left(\frac{\tilde{\mathbf{0}}}{\rho_0} \tau_\alpha \gamma_\alpha \frac{\partial}{\partial \xi_\alpha} + \nabla \cdot \left(\frac{\partial \psi}{\partial \nabla \xi_\alpha} \right) - \frac{\partial \psi}{\partial \xi_\alpha} \right); \\
&L_\alpha^\xi(\eta) = L_\alpha^A + (L_\alpha^M - L_\alpha^A)\eta^2(3-2\eta); \\
&\tau_\alpha = \boldsymbol{n}^\alpha \cdot \boldsymbol{F}_p \cdot \boldsymbol{P}^T \cdot \boldsymbol{F}_e \cdot \boldsymbol{U}_t \cdot \boldsymbol{m}^\alpha,
\end{aligned} \tag{10}$$

where P=$\rho_0 J_e F_e$. $\partial\psi/\partial E_e$. U_t^{-1} . F_p^{T-1} is the first Piola-Kirchhoff stress; $L_\alpha{}^A$ and $L_\alpha{}^M$ are the kinetics coefficients for dislocations in A and M, respectively. Momentum balance equation is expressed as $\nabla.P=0$. The boundary conditions for PTs and dislocations are $\nabla\eta \cdot k$=0 and $\nabla\xi_\alpha \cdot b^\alpha$=0, respectively, where k is the unit normal.

3- Numerical Solutions

FEM approach and code COMSOL with embedded remeshing procedure have been utilized. Plane strain problems and straight edge dislocations are considered. All size and time parameters are normalized by 1nm and 1ps, respectively. All results are shown in the deformed configuration. The following material parameters are used unless stated different [11,12]: H=0.7nm, $|b|$=0.35nm, $\beta_\xi{}^A$=$\beta_\xi{}^M$=7.5 ×10^{-11} N, $A_\alpha{}^M$=3$A_\alpha{}^A$=2.25GPa, γ_α=0.5, $\beta_\xi{}^A$=$\beta_\xi{}^M$=2.59×10^{-10} N, $L_\alpha{}^A$=$L_\alpha{}^M$=2600(Pa·s)$^{-1}$, A_0=20.6MPa/K, Δs=5.05MPa/K, θ=298K, θ_c=-90K, θ_e=100K, a=4, ε_t^x=ε_t^y=-0.05, ε_t^{xy}=0.1, shear modulus μ=71.5 GPa, bulk modulus K=112.6 GPa. To validate the numerical procedure, it is found that the results well match the local thermodynamic equilibrium condition and the interfaces well coincide with the equilibrium contours [18].

3- 1- The evolution of dislocations and high-pressure phase in a nanograined material under pressure and shear

For the chosen material parameters, the phase equilibrium pressure between the low and high-pressure phases is 10 GPa. With one dislocation, PT starts and occurs to a significant extent at hydrostatic pressure of P_h=15 GPa. A rectangular sample with the size of 50×20 is considered which includes two nanograins surrounded by two areas at the top and bottom of the sample, each with the size of 50×5, which plays a role as elastic accommodators (Fig. 1). A horizontal dislocation band is located in the middle of the left grain. Two dislocation systems inclined at ±30° from the horizontal line are located in the right grain. The lower side of the sample is fixed in both directions, the periodic boundary conditions are applied at the lateral sides, and a vertical stress is applied to the upper side in the deformed state, which results in the initial average pressure in the nanograins. The upper side is also subjected to a horizontal displacement u (which is given in terms of prescribed macroscopic shear γ=u/h, with the height of grains h=20). In the first problem, dislocation activity in the right grain is forbidden. Under the applied shear, the dislocations of opposite signs are nucleated from both grain boundaries

in the left grain and create dislocation pile ups. The pile-ups produce strong concentration of the stress tensor near their tips, which significantly increase the local transformation work. Thus, the external pressure required for PT can be drastically decreased. For example, in this problem due to the generation of 3 dislocation piled ups due to applied γ=0.2, the PT pressure is reduced from P_h=15 GPa to 1.2 GPa (an averaged pressure over grains after PT). This explains drastic reduction of the PT pressure due to the applied shear in experiments for various materials [2, 3]. Figs. 2(a) and 2(b) show the coupled solutions for PT and dislocations at some initial stages (t=0.5) and the stationary solutions in the right grain, respectively. The phase concentration, i.e. the ratio of the transformed area to the initial area in the right grain, reaches c=0.51. Such a significant transformation progress is due to the small distance between stress concentrators, which leads to a coalescence of nuclei and corresponding morphological transition.

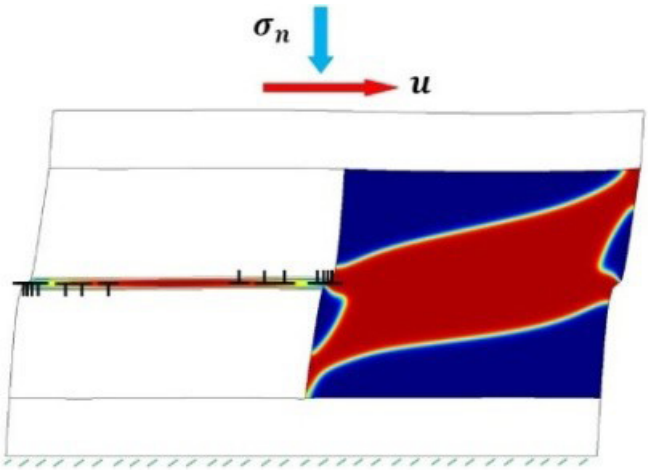

Fig. 1. Schematics of the sample under pressure and shear and stationary solution. Dislocations in the left grain cause transformation from the low-pressure (blue) to the high (red) pressure phases.

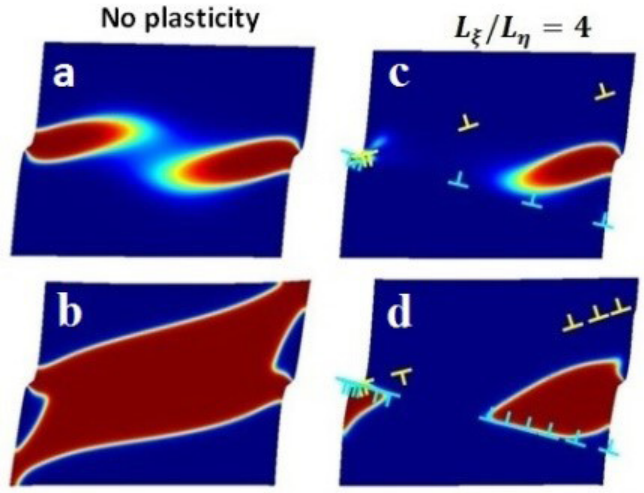

Fig. 2. The solution for PT without plasticity in the right grain at t=0.5 (a) and for the stationary state (b). The coupled PT and dislocation solutions at t=0.5 (c) and for the stationary state (d).

When dislocations in the right grain are included, in addition to the promoting effect of plasticity on PT, it also suppresses PT by relaxing stresses at other concentrators. The solutions for PT and dislocations with two dislocation systems in the transformed grain are presented in Figs. 2(c) and 2(d). Several dislocations nucleated at the tip of the pileup and propagated through the right grain. Due to stress relaxation, almost no high-pressure phase appears at the left side of the right grain. For the same reason, PT is also suppressed in the right side of the right grain and the transformed region (Fig. 2(c)) is smaller than that in Fig. 2(b). Therefore, while the number of dislocations increases, coalescence does not occur and the stationary solution is reached with c=0.19 and 6 and 3 dislocations in the lower and the upper dislocation systems, respectively.

3- 2- Growth and arrest of a martensitic plate.

A rectangular sample with the size of 67×20 is considered, which is divided into two grains. The transformation strain in the right grain is rotated by 15° counter clockwise with respect to the left grain. The lower and upper straight sides are fixed in the y direction; the lateral sides are stress-free. A martensitic rectangular nucleus with the size of 5×3 is initially located at the lower left corner of the sample. Two dislocation systems inclined at ±60° are included in the left grain with initial conditions ξ_α=0.01. The sample is initially stress-free and subjected to uniform cooling. The following material parameters are used [12]: A_0=4.4MPa/K, θ_c=-183K, θ_e=215K, a=3, ε_t^x=0, ε_t^{xy}=-0.13, ε_t^y=0.137 for the left grain, and ε_t^x=0.063, ε_t^{xy}=-0.147, ε_t^y=0.074 for the right grain. Without plasticity, the M propagates through the entire left grain and below the critical temperature T=50K, the M plate passes through the grain boundary and propagates through the entire right grain (Fig. 3(a)). With plasticity, dislocation pairs in both slip planes nucleate at the tip of the growing plate. For the coupled dislocations and PT problem, dislocations of one sign propagate toward upper boundary of the sample and dislocations of the opposite sign remain within the M plate. For 40 < T < 50 K, the M plate is arrested by one dislocation in the middle of a sample (Fig. 3(b)). This results in an athermal friction of 10 K in terms of overcooling temperature. For T < 40 K, the growth continues through the right grain similar to that of Fig. 3(a). The obtained results are in qualitative agreement with experiments on plate-lath martensite morphological transition due to plastic M growth [4].

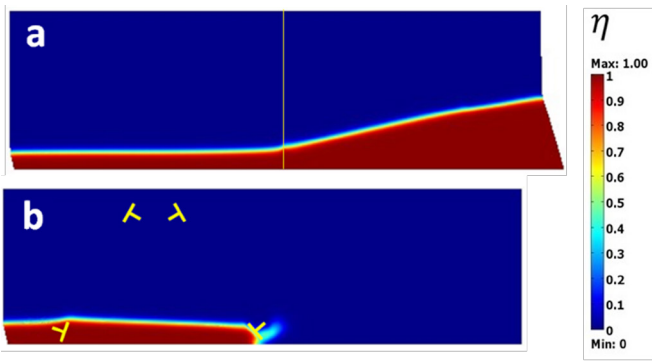

Fig. 3. Stationary solutions for (a) completed martensitic plate without dislocations at T=50K and (b) arrested martensitic plate due to dislocations in the left grain at T=50K.

To summarize, a PFA to the interaction between PTs and dislocations at large strains is presented, including the following main features of the interaction event: (a) multiplicative kinematic decomposition of the deformation gradient into elastic, transformational, and plastic contributions; (b) inheritance of dislocations of austenite in martensite during martensitic PT and dislocations of martensite in austenite during reverse PT; (c) dependence of all material parameters for dislocations on the order parameters for PT. Problems for temperature and stress-induced PTs interacting with dislocation evolution are solved and several effects, including the dual effect of plasticity on PT and athermal interface resistance caused by dislocations are presented. A similar approach can be developed for the interaction of dislocations with twins and diffusive PTs, as well as electromagnetic and reconstructive PTs. For multivariant martensitic PTs, the thermodynamic potential should include a thermodynamically consistent expression for interface tension (stresses) [14-16] and a mixed term of the gradients of different order parameters which allows us to control the energy of a martensite-martensite interface independent of the energy of the austenite-martensite interface. Also, the effect of the variable surface energy and finite width of the external surface should be included [17], which may lead to multifaceted effects similar to those revealed in [17] without plasticity.

Acknowledgements

The supports of Isfahan University of Technology and Iowa State University are gratefully acknowledged.

References

[1] F. D. Fischer, G. Reisner, E. Werner, K. Tanaka, G. Cailletaud, T. Antretter, A new view on transformation induced plasticity (TRIP), *Int J Plast*, 16 (2000) 723-748.

[2] V. I. Levitas, Continuum mechanical fundamentals of mechanochemistry, In: Ed. Y. Gogotsi and V. Domnich, High Pressure Surface Science and Engineering. Section 3, *Institute of Physics Publishing*, 159-292, 2004.

[3] V. I. Levitas, High-pressure mechanochemistry: conceptual multiscale theory and interpretation of experiments, *Phys Rev B*, 70 (2004) 184118.

[4] G. B. Olson, M. Cohen, Dislocation theory of martensitic transformations, In: Ed. F R N. Nabarro, *Dislocations in solids*, Amsterdam, North-Holland, 297-407, 1998.

[5] V. I. Levitas, Structural changes without stable intermediate state in inelastic material. Parts I and II, *Int. J. Plast*, 16 (2000) 805-849 and 851-892.

[6] A. V. Idesman, V. I. Levitas, E. Stein, Structural changes in elastoplastic materials: a unified finite element approach for phase transformation, twinning and fracture, *Int. J. Plast*, 16 (2008) 893-949.

[7] Y. Wang, A. G. Khachaturyan, Multi-scale phase field approach to martensitic transformations, *Mater Sci Eng A*, 438&440 (2006) 55-63.

[8] J. Kundin, D. Raabe, H. Emmerich, A phase-field model for incoherent martensitic transformations including plastic accommodation processes in the austenite, *J Mech Phys Solids*, 59 (2011) 2082-2102.

[9] V. I. Levitas, M. Javanbakht, Advanced phase field approach to dislocation evolution, *Phys Rev B*, 86 (2012) 140101.

[10] V. I. Levitas, Phase-field theory for martensitic phase transformations at large strains, *Int J Plast*, 49 (2013) 85-118.

[11] V. I. Levitas, M. Javanbakht, Phase transformations in nanograin materials under high pressure and plastic shear: nanoscale mechanisms, *Nanoscale*, 6 (2014) 162-166.

[12] V. I. Levitas, M. Javanbakht, Phase field approach to interaction of phase transformation and dislocation evolution, *Appl Phys Lett*, 102 (2013) 251904.

[13] Y. U. Wang, Y. M. Jin, A. M. Cuitino, A. G. Khachaturyan, Application of phase field microelasticity theory of phase transformations to dislocation dynamics: model and three-dimensional simulations in a single crystal, *Philos Mag*, 81 (2001) 385-393.

[14] V. I. Levitas, M. Javanbakht, Surface tension and energy in multivariant martensitic transformations: phase-field theory, simulations, and model of coherent interface, *Phys Rev Lett*, 105 (2011) 165701.

[15] V. I. Levitas, M. Javanbakht, Phase-field approach to martensitic phase transformations: effect of martensite-martensite interface energy, *Int J Mat Res*, 102 (2011) 652-665.

[16] V. I. Levitas, Phase field approach to martensitic phase transformations with large strains and interface stresses, *J. Mech Phys Solids*, 70 (2014) 154-189.

[17] V. I. Levitas, M. Javanbakht, Surface-induced phase transformations: multiple scale and mechanics effects and morphological transitions, *Phys Rev Lett*, 107 (2011) 175701.

[18] M. Javanbakht, V. I. Levitas, Interaction between phase transformations and dislocations at the nanoscale. Part 2: Phase field simulation examples, *J Mech Phys Solids*, 82 (2015) 164-185.

Please cite this article using:

M. Javanbakht and V. I. Levitas, Phase Field Method to the Interaction of Phase Transformations and Dislocations at Nanoscale, *AUT J. Mech. Eng.*, 1(2) (2017) 243-246.

DOI: 10.22060/mej.2017.11892.5209